

Implementation of PI controller for fourth order Resonant Power Converter with capacitive output filter

R. Geetha¹, Dr.T.S. Sivakumaran²

¹(Research Scholar, Bharath University, Chennai, India)

²(Dean PG Studies, Arunai College of Engineering, Tiruvannamalai, India)

Abstract: A closed loop control of the fourth order (LCLC configuration) resonant converter has been simulated and presented in this paper. The PI controller has been used for closed loop operation and the performance of proposed converter has been estimated with the closed loop and the open loop condition. The steady state-transient responses of nominal load, sudden line and load disturbances have been obtained to validate the controller performance. The proposed approach is expected to provide better voltage regulation for dynamic load conditions.

Keywords: Resonant Power Converter, LCLC configuration, PI Controller, State Space analysis

I. Introduction

The increasing efforts on pushing to high power density and high efficiency DC/DC converter have lead us to develop converters capable of operating at higher switching frequency with high efficiency. For this reason, resonant converters have made lots of attentions due to high efficiency, high switching frequency and high power density. The invention and evolution of various DC–DC resonant converters (RC) have been focused for telecommunication and aerospace applications in the recent past. It has been set up that these converters experience high switching loss, reduced reliability, increased electro-magnetic interference (EMI) and high acoustic noise at high frequencies [1-12]. The LCLC resonant inverter is a fourth order resonant topology which has been successfully used in different industrial applications such as space power distribution systems, resonant inverters, Ion generator power supplies, multi lamp operation ballasts, renewable energy power conditioning systems, constant-current power supplies and dual-output resonant converters [13-19]. This topology employs more parasitic elements and has many desirable features. Thus, it appears to be a serious prospect for high voltage conversion [20-25]. The converter of this topology uses an inductive output filter similar to a Parallel Resonant Converter (PRC) [1, 2]. In [12], [26] LCLC resonant converters with an LC output filter are analyzed using the First Harmonic Approximation technique (FHA). In high voltage applications, a resonant converter with a capacitive output filter is used, because the inductor in an output filter is bulky and very difficult to fabricate [20]–[25].

II. Resonant Converters

Resonant converters contain resonant L-C networks whose voltage and current waveforms vary sinusoidally during one or more subintervals of each switching period. The resonant network has the effect of filtering higher harmonic voltages such that a nearly sinusoidal current appears at the input of the resonant network [4]. There are three main types of resonant networks, which are shown in Fig. 1.

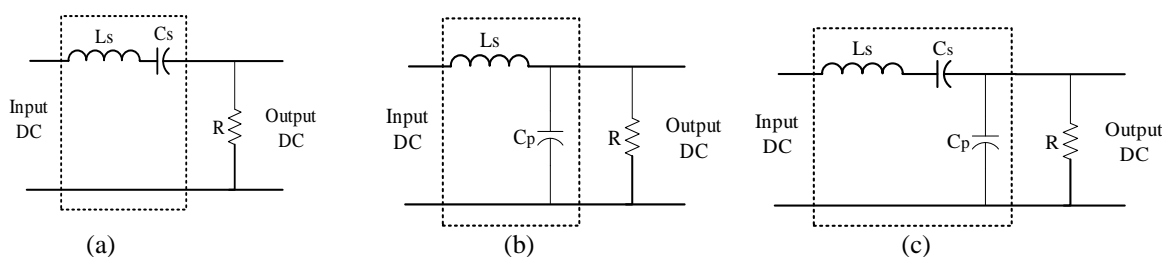


Fig. 1. Resonant networks: (a) Series Resonant; (b) Parallel Resonant; (c) Series- Parallel Resonant.

Series resonant, parallel resonant and series-parallel resonant [26]. Depending on how the resonant networks are combined with other circuit configurations, one can obtain several types of resonant converters. The more common configurations are: DC-to-high-frequency-AC inverters, resonant DC-DC converters and resonant link converters. In this work, the focus will be on the resonant DC-DC converters.

A main advantage of resonant converters is the reduced switching losses. Resonant converters can run in either the zero-current-switching (ZCS) or zero-voltage-switching (ZVS) mode [27]. That means that turn-on or turn-off transitions of semiconductor devices can occur at zero crossings of tank voltage or current waveforms, thus reducing or eliminating some of the switching loss mechanisms. Since the losses are proportional to switching frequency, converters can operate at higher switching frequencies than comparable PWM converters [28].

1. Series Parallel Resonant Converters (SPRC)

The closed loop control of series-parallel resonant DC-DC converter (LCLC) with capacitive output filter is shown in Fig. 2.

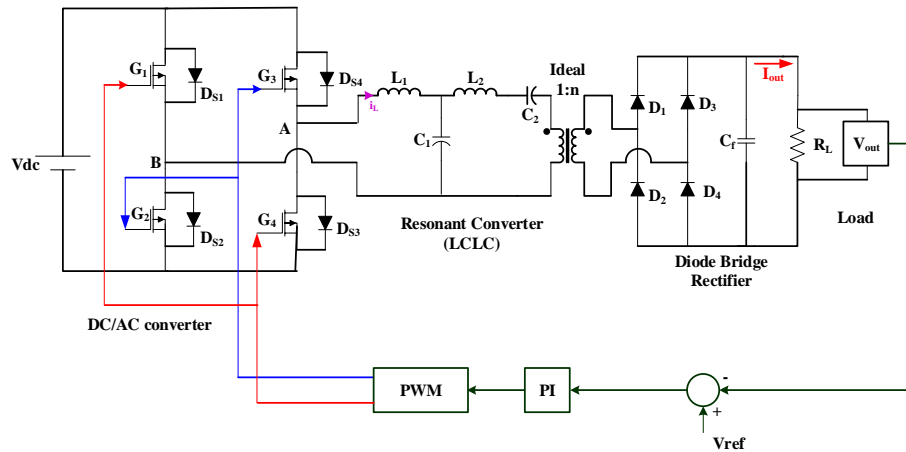


Fig. 2 closed loop control of resonant converter with LCLC configuration

This converter has also been often used with inductive output filter [29], [4]. However, in the current work the focus will be on the converter with capacitive output filter because this configuration is better suited for high-voltage applications. Eq. (1) gives the voltage conversion ratio of the series-parallel resonant converter.

$$\frac{V_o}{nV_{in}} = \frac{4}{\pi} \cdot \frac{k_{21}}{k_v} \tag{1}$$

$$k_{21} = \frac{1}{\sqrt{\left[1 - \alpha \cdot (f_{s,N}^2 - 1) \cdot \left(1 + \frac{\tan(\beta)}{\omega C_p R_e}\right)\right]^2 + \left[\alpha \cdot (f_{s,N}^2 - 1) \cdot \frac{1}{\omega C_p R_e}\right]^2}}$$

$$k_v = 1 + 0.27 \cdot \sin\left(\frac{\theta}{2}\right)$$

Where

- $\alpha = C_p / C_s$ - Ratio of the parallel to the series capacitor
- θ - Output rectifier conduction angle
- β - Phase displacement of the fundamentals of the voltage across the parallel capacitor and the input current of the output rectifier
- $\omega C_p R_e$ - Dimensionless parameter
- n - Transformer turns ratio
- $f_{s,N} = f_s / f_o$ - Normalized switching frequency
- f_s - Switching frequency
- $f_o = (2\pi\sqrt{L_s C_s})^{-1}$ - Series resonant frequency

This converter operates for low power close to the parallel resonant frequency $(2\pi\sqrt{L_p C_s})^{-1}$ and for full load, close to the series resonant frequency $(2\pi\sqrt{L_s C_s})^{-1}$. The real resonant frequency of the circuit changes with the load as shown in Fig.3. This happens because the load defines the influence of C_p on the resonant frequency. For high load the resonant current flows for only a small part of the switching period through C_p . Thus, the converter behaves as a series resonant converter and the resonant frequency is almost equal the series resonant

frequency f_0 . On the other hand, for low load the resonant current flows almost the whole switching period through C_p . Therefore, the converter behaves as a parallel resonant converter. When operating above resonance, the converter behaves as a series resonant converter at lower frequencies (high load operation) and as a parallel resonant converter at higher frequencies (low load operation) [30]. At higher switching frequencies the series capacitance becomes so small that it behaves just as a DC blocking capacitance.

The resonant inductor then resonates with the parallel capacitor and the converter operates in the parallel resonant mode [31]. By proper selection of the resonant elements, the series-parallel resonant converter has better control characteristics than the resonant converters with only two resonant elements [32] being less sensitive to component tolerances. This configuration aims to take advantage of the desirable characteristics of the series and the parallel converter while reducing or eliminating their drawbacks. Unlike the series resonant converter, the series-parallel resonant converter is capable of both step-up and step-down operation [33]. This capability can be observed in the voltage conversion ratio curves of the series-parallel resonant converter as shown in Fig. 3.

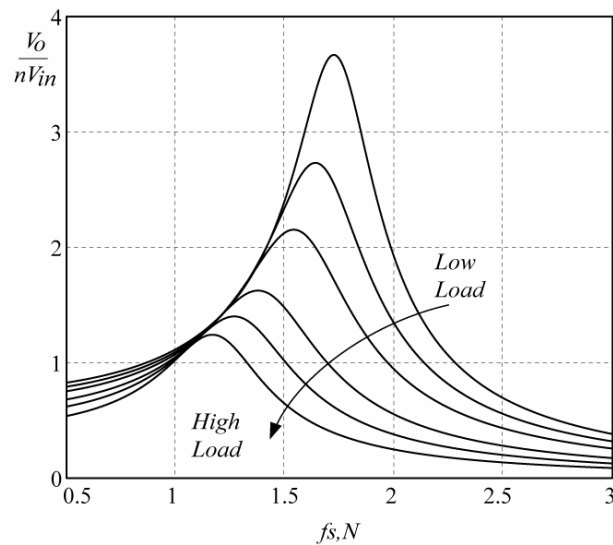


Fig. 3 Voltage conversion ratio of a series-parallel resonant converter independency on the load and on the normalized switching frequency

The voltage conversion ratio curves also show that the output voltage can be regulated at no load. Thus, the main disadvantage of the series resonant converter is successfully eliminated with this configuration. It is important to note that the lower the value of the parallel resonant capacitor C_p the more the circuit will have the characteristic of a series resonant converter. Therefore, the value of the parallel resonant capacitor C_p may not be too low in order to permit that the converter takes the characteristic of the parallel resonant converter at light load. When the resonant current flows for a long interval of the switching period through C_p (and this is the case at light load operation), it is increased above the level expected in the series resonant converter, producing a higher output voltage. Therefore the presence of C_p in combination with L_s results in boosting of the converter output voltage at light load [33].

The main disadvantage of the parallel resonant converter, i.e. the high device current independent on the load is supposed to be eliminated in the series-parallel resonant converter. Unfortunately this drawback cannot be totally removed but, with the proper choice of the resonant elements, it can be considerably reduced for certain load levels [29], [26]. The limiting factor in reducing C_p , to reduce circulating current is the upper switching frequency limit. As the value of C_p gets lower relative to C_s , the ratio $\alpha = C_p/C_s$ also gets lower and consequently the converter operating frequency range gets wider. As very high switching frequencies are not desirable due to practical implementation limitations, one has to find a compromise between reducing the circulating current for low loads and having a reasonable limit for the upper switching frequency. Normally one designs the converter such that it operates essentially as a series resonant converter so that the circulating current will decrease as the load decreases to a certain level. Below this level, the converter behaves like a parallel resonant converter, and the circulating current no longer decreases with load [4]. Unfortunately, in the case of high-voltage generation, where high voltage conversion ratio is required, the value of C_p cannot be significantly reduced. Thus, the circulating current does not decrease considerably with the load and losses remain almost unchanged.

III. Modelling of LCLC Resonant Converter

The equivalent circuit of LCLC resonant converter is shown on in Fig.2. The mathematical model using obtained assuming all the components to be ideal.

The state space equation for the proposed converter is given by

$$\dot{X} = AX + BU \tag{2}$$

Where,

$$\dot{X} = \frac{d}{dt} \begin{bmatrix} iL_1 \\ vC_1 \\ iL_2 \\ vC_2 \end{bmatrix}, \quad X = \begin{bmatrix} iL_1 \\ vC_1 \\ iL_2 \\ vC_2 \end{bmatrix}, \quad U = \begin{bmatrix} V_i \\ V_o \end{bmatrix}$$

The state space equation for LCLC resonant converter is get from Fig.2.

$$\begin{aligned} \frac{diL_1}{dt} &= m \frac{V_i}{L_1} - \frac{vC_1}{L_1} \\ \frac{dvC_1}{dt} &= \frac{1}{C_1}(iL_1 - iL_2) \\ \frac{diL_2}{dt} &= \frac{1}{L_2}(vC_1 - vC_2) \\ \frac{dvC_2}{dt} &= n \frac{V_o}{C_2} - \frac{iL_2}{C_2} \end{aligned} \tag{3}$$

From equations (2) and (3), we can get,

$$\frac{d}{dt} \begin{bmatrix} iL_1 \\ vC_1 \\ iL_2 \\ vC_2 \end{bmatrix} = \begin{bmatrix} 0 & -\frac{1}{L_1} & 0 & 0 \\ \frac{1}{C_1} & 0 & -\frac{1}{C_1} & 0 \\ 0 & \frac{1}{L_1} & 0 & -\frac{1}{L_2} \\ 0 & 0 & -\frac{1}{C_2} & 0 \end{bmatrix} \begin{bmatrix} iL_1 \\ vC_1 \\ iL_2 \\ vC_2 \end{bmatrix} + \begin{bmatrix} -\frac{1}{L_1} & 0 \\ 0 & 0 \\ 0 & 0 \\ 0 & -\frac{1}{L_2} \end{bmatrix} \begin{bmatrix} V_i \\ V_o \end{bmatrix} \tag{4}$$

From equation (4), we get,

$$A = \begin{bmatrix} 0 & -\frac{1}{L_1} & 0 & 0 \\ \frac{1}{C_1} & 0 & -\frac{1}{C_1} & 0 \\ 0 & \frac{1}{L_1} & 0 & -\frac{1}{L_2} \\ 0 & 0 & -\frac{1}{C_2} & 0 \end{bmatrix}, \quad B = \begin{bmatrix} -\frac{1}{L_1} & 0 \\ 0 & 0 \\ 0 & 0 \\ 0 & -\frac{1}{L_2} \end{bmatrix}$$

IV. Control Strategy of LCLC Resonant Converter

Fig.2 shows a typical structure of LCLC-SPRC with capacitive output filter. In dc/dc conversion application, the output filter can be either an LC network or a single capacitor. Considering the demand for shrinking the volume and reducing the insulation cost in high voltage application, a unitary capacitor filter is usually utilized. In the resonant tank, the Cp will be clamped by the parallel connected filter capacitor Cf when the rectifier conducts. And the natural resonance is only constituted by Ls, Cs. After the rectifier turns OFF, the Cp detaches from Cf and joins into the resonance. Such a complex behavior may take place in one switching period, deepening the hardness to establish the model which could reflect the exact operation characteristics of the converter.

The inverter consists of four MOSFETs S1–S4, and the fast recovery diodes D1–D4 are used to organize the full-bridge rectifier. For simplification, the transformer turn ratio is set to 1:1, and some basic assumptions are made as follows [34-35]. The conduction of S1 and S4 in the inverter or D1 and D4 in the rectifier is defined as positive conduction and the conduction of S2, S3 in the inverter or D3, D2 in the rectifier is defined as negative conduction.

The PI controller used to tune the gate pulses of the inverter MOSFETs corresponding to the load with respect to the reference voltage. The pulse generation using PI controller as shown in Figs. 4 and 5.

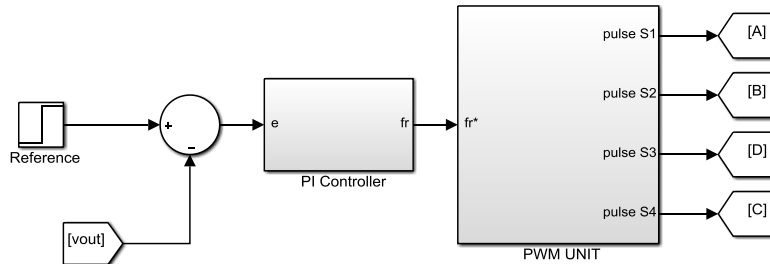


Fig. 4 PWM generation with PI controller

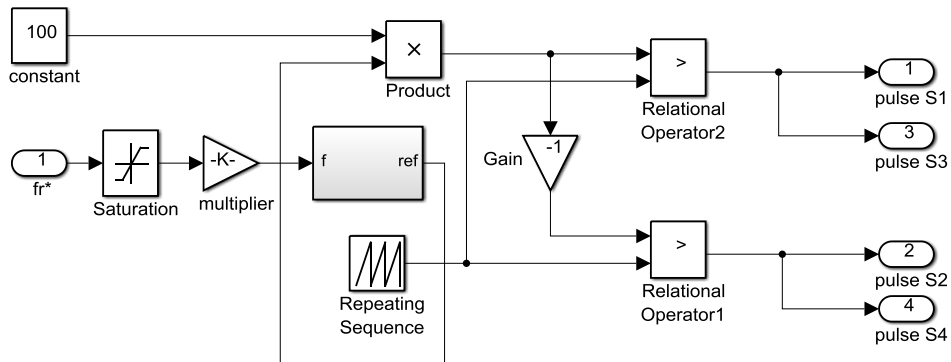


Fig. 5 PWM pulse generator

V. Simulation Results and Discussion

The performance analysis of the proposed LCLC resonant power converter has been tested with MATLAB/Simulink software platform. Zero voltage and Zero current switching time are obtained through simulation for the proposed converter. When the switching frequency is higher than resonant frequency, the voltage gain of LCLC converter is always less than one, and it operates as a resonant converter and zero voltage switching (ZVS) can be achieved. When the switching frequency is lower than resonant frequency, for different load conditions, both ZVS and zero current switching (ZCS) could be achieved. The Simulink diagram of the closed loop LCLC resonant power converter with PI controller is shown in Fig.6. The servo and regulatory responses of the proposed converter has been taken and the results are shown in Figs. 7-10.

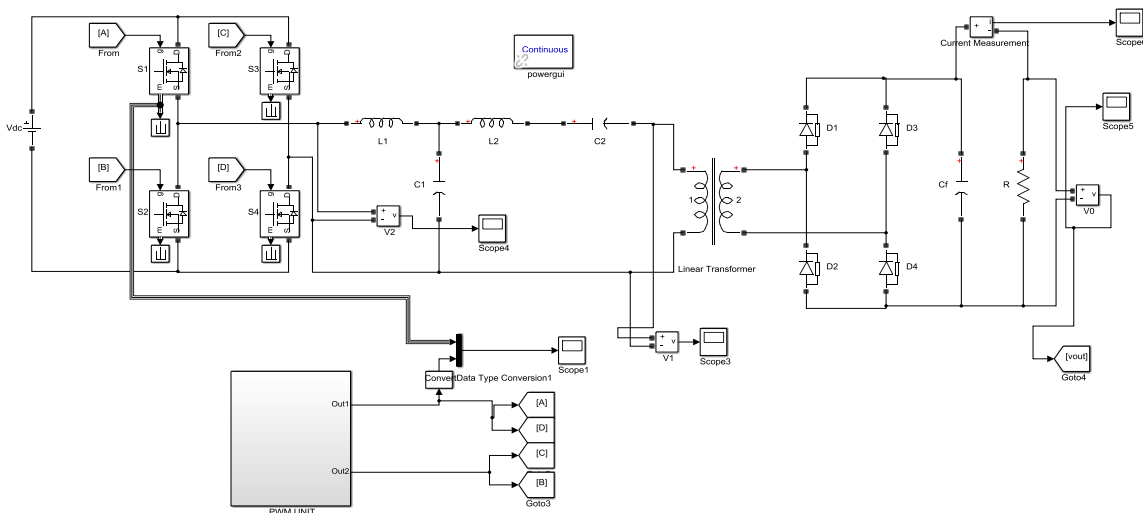


Fig. 6 Matlab Simulink model of the proposed LCLC Resonant converter with closed loop operation

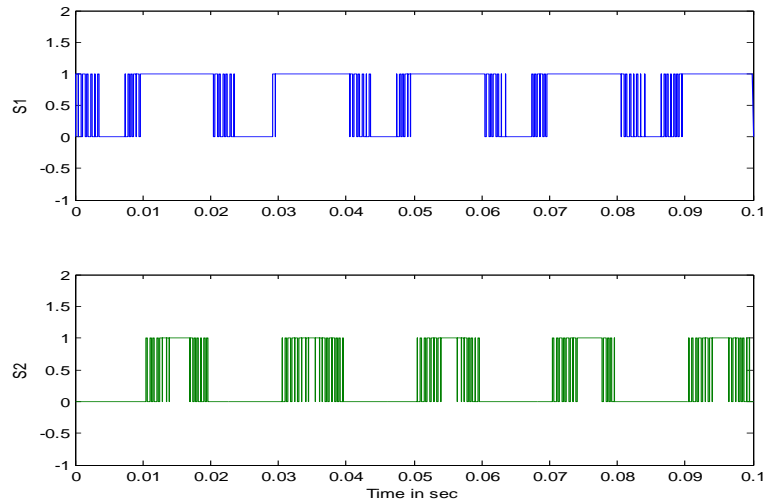


Fig. 7 Switching pulses for S1 and S2

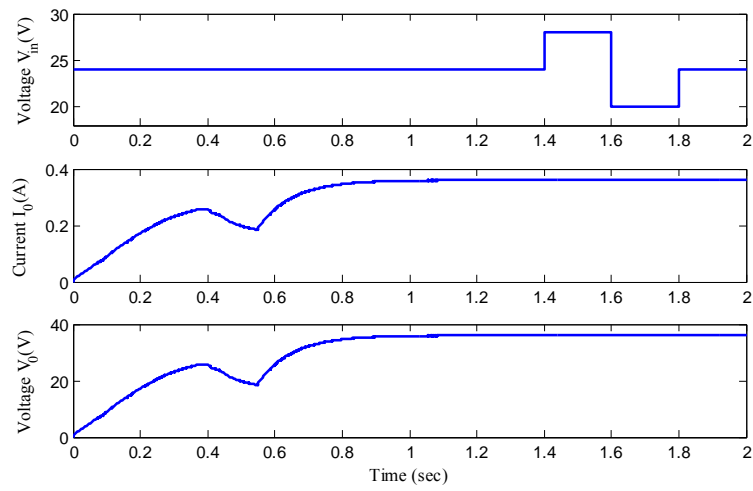


Fig. 8 Input and output responses of LCLC-SPRC with PI controller

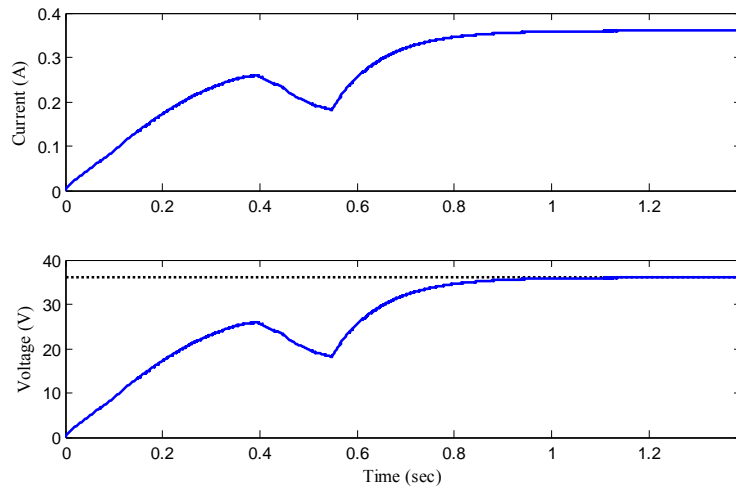


Fig. 9 Output voltage and current responses of LCLC –SPRC at initial condition

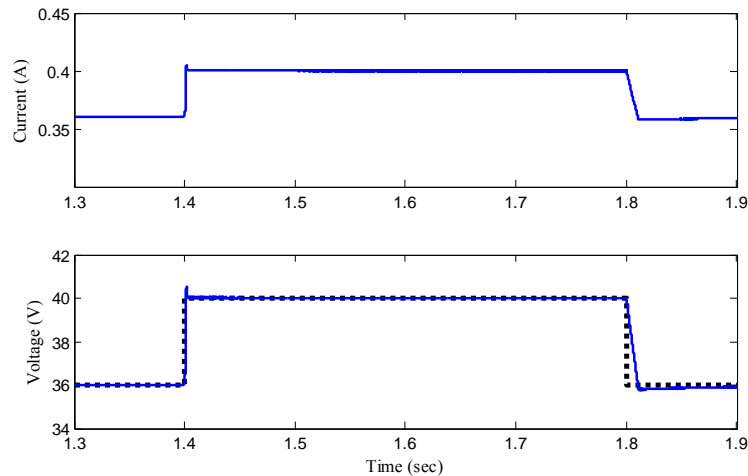


Fig.10 Output voltage and current responses of LCLC-SPRC with load changes

Fig.7 shows the zero voltage and zero current switching responses of switches S1 and S2 of the LCLC-SPRC power converter. Fig.8 shows the input and output voltage and current responses of LCLC-SPRC with PI controller. The servo response of the LCLC converter with PI controller has been observed from the figure 8. It represents the input voltage suddenly incremented from 24V to 28V at $t=1.4$ sec and suddenly decremented to 20V at 1.6 sec and return back to the actual input voltage of 24V at 1.8 sec. During this time period of $t=1.4 - 1.8$ Sec the output does not vary due to servo disturbance and the boosted output voltage is held as constant of 38V. Fig.9 shows the output voltage and current responses of LCLC –SPRC at initial condition. Fig.10 shows the output voltage and current responses of LCLC-SPRC with load changes. During this regulatory response, the converter output voltage has been quickly settled with its reference value without any fluctuation with load increment at $t=1.4$ and load decrement at 1.8 sec.

VI. Conclusion

In this paper, a new LCLC configuration is proposed by using state space analysis. The output voltage and current are obtained using zero voltage and zero current switching time using PI controller. The steady-state solutions have been deduced and simplified by introducing the output voltage coefficient. The reaction time of resonant current has been calculated using output voltage coefficient, indicating a frequency limit that takes in the converter to operate in CCM. From the simulation results, it is apparent that the proposed LCLC resonant power converter has reached its steady state response without any oscillations with implementation of PI controller. In time to come it may continue the operation of LCLC-SPRC with fuzzy and neural controllers and compare the performance about the same.

References

- [1]. M.K. Kazimierzczuk and D. Czarkowski, Resonant Power Converters (JohnWiley and Sons Inc., 1995).
- [2]. R.W. Erickson, Fundamentals of Power Electronics (Kluwer Academic Publishers, 1997).
- [3]. I Batarseh, Resonant converter topologies with three and four energy storage elements, IEEE Trans. Power Electron, 9(1), 1994, 64-73.
- [4]. R L Steigerwald, A comparison of half-bridge resonant converter topologies, IEEE Trans. Power Electron, 3(2), 1988, 174-182.
- [5]. A K S Bhat, Fixed-frequency PWM series-parallel resonant converter, IEEE Trans. Ind. Appl, 28(5), 1992, 1002-1009.
- [6]. H. I. Sewell, M. P. Foster, C. M. Bingham, D. A. Stone, D. Hente, and D. Howe, Analysis of voltage output LCC resonant converters, including boost mode operation, IEE Proc. Electronics Power Application, 2003, 673-679.
- [7]. J A Martin-Ramos, J. Diaz, A. M. Pernia, J. M. Lopera, and F. Nuno, Dynamic and steady-state models for the PRC-LCC resonant topology with a capacitor as output filter, IEEE Trans. Ind. Electron, 54(4), 2007, 2262-2275.
- [8]. Y. A. Ang, C. M. Bingham, M. P. Foster, D. A. Stone, and D. Howe, Design oriented analysis of fourth-order LCLC converters with capacitive output filter, IEE Proc. Electronic Power Application, 2005, 310-322.
- [9]. J L Sosa, M. Castilla, J. Miret, L. G. Vicuna, and J. Matas, Modeling and performance analysis of the DC/DC series-parallel resonant converter operating with discrete self-sustained phase-shift modulation technique, IEEE Trans. Ind. Electron, 56(3), 2009, 697-705.
- [10]. M Borage, K. V. Nagesh, M. S. Bhatia, and S. Tiwari, Design of LCL-T resonant converter including the effect of transformer winding capacitance, IEEE Trans. Ind. Electron, 56(5), 2009, 1420-1427.
- [11]. E H Kim and B. H. Kwon, Zero-voltage- and zero-current-switching full-bridge converter with secondary resonance, IEEE Trans. Ind. Electron, 57(3), 2010, 1017-1025.
- [12]. J H Cheng and A. F. Witulski, Analytic solutions for LLC parallel resonant converter simplify use of two-and three-element converters, IEEE Trans. Power Electron, 13(2), 1998, 235-243.
- [13]. P K Jain and M. C. Tanju, A unity power factor resonant AC/DC converter for high-frequency space power distribution system, IEEE Trans. Power Electron, 12(2), 1997, 325-331.

- [14]. Z Ye, P. K. Jain and P. C. Sen, A two-stage resonant inverter with control of the phase angle and magnitude of the output voltage, *IEEE Trans. Ind. Electron*, 54(5), 2007, 2797-2812.
- [15]. W. G. Chen, Y. H. Rao, C. H. Shan, G. Fujita, and T. Yasutoshi, The design and experiment of Ion Generator power supply for Vacuum Sputtering, in *Proc. IEEE PCC*, 2007, 931-935.
- [16]. C. Liu, F. Teng, C. Hu, and Z. Zhang, LCLC resonant converter for multiple lamp operation ballast, in *Proc. IEEE APEC*, 2003, 1209-1213.
- [17]. A. Conesa, G. Velasco, H. Martinez, and M. Roman, LCLC resonant converter as maximum power point tracker in PV systems, in *Proc. IEEE EPE*, 2009, 1-9.
- [18]. M Borage, S. Tiwari, and S. Kotaiah, Analysis and design of an LCLT resonant converter as a constant-current power supply, *IEEE Trans. Ind. Electron*, 52(6), 2005, 1547-1554.
- [19]. Y. Ang, C. M. Bingham, M. P. Foster and D. A. Stone, Analysis and control of dual-output LCLC resonant converters, and the impact of leakage inductance, in *Proc. IEEE PEDS*, 2007, 145.150.
- [20]. J A Martin-Ramos, A. M. Pernia, J. Diaz, F. Nuno, and J. A. Martinez, Power supply for a high-voltage application, *IEEE Trans. Power Electron*, 23(4), 2008, 1608-1619.
- [21]. J Biela and J. W. Kolar, Using transformer parasitics for resonant converters—a review of the calculation of the stray capacitance of transformers, *IEEE Trans. Ind. Appl*, 44(1), 2008, 223-233.
- [22]. C Iannello, S. Luo, and I. Batarseh, Full bridge ZCS PWM converter for high-voltage high-power applications, *IEEE Trans. Aerosp. Electron. Syst*, 38(2), 2002, 515-526.
- [23]. C. B. Viejo, M. A. P. Garcia, M. R. Secades, and J. U. Antolin, A resonant high voltage converter with C-type output filter, in *Proc. IEEE IAS*, 1995, 2401-2407.
- [24]. J. A. Pomilio and C. J. B. Pagan, resonant high-voltage source working at resonance for pulsed laser, in *Proc. IEEE PESC*, 1996, 1627-1632.
- [25]. V. Garcia, M. Rico, J. Sebastian, M. M. Hernando, and J. Uceda, An optimized DC-to-DC converter topology for high-voltage pulse-load applications, in *Proc. IEEE PESC*, 1994, 1413-1421.
- [26]. M.H. Rashid, *Power Electronics Handbook* (Academic Press, San Diego,CA, 2001).
- [27]. R. L. Steigerwald, *Power Electronic Converter Technology*. *Proc. of the IEEE*, 2001, 890 – 897.
- [28]. R.W. Erickson and D. Maksimovic, *Fundamentals of Power Electronics* (Second Edition, Kluwer Academic Publishers, 2001).
- [29]. A K S Bhat, A Resonant Converter suitable for 650 V DC Bus Operation. *IEEE Transactions on Power Electronics*, 6(4), 1991, 739 – 748.
- [30]. G. D. Demetriades, P. Ranstad and C. Sadarangari, Three Elements Resonant Converter: the LCC topology by using MATLAB. 31st Annual IEEE Power Electronics Specialists Conference, Galway, Ireland, 2000, 1077 – 1083.
- [31]. R W Erickson, S. D. Johnson and A. F. Witulski, Comparison of Resonant Topologies in High-Voltage DC Applications. *IEEE Transactions on Aerospace and Electronic Systems*, 24(3), 1988, 263-274.
- [32]. I Bartaseh, Resonant Converter Topologies with Three and Four Energy Storage Elements. *IEEE Transactions on Power Electronics*, 9(1), 1994, 64 – 73.
- [33]. A. J. Forsyth and S. V. Mollov, Simple Equivalent Circuit for the Series-Loaded Resonant Converter with Voltage Boosting Capacitor. *IEE Proc. Electric Power Applications*, 1998, 301 – 306.
- [34]. G Ivensky, A. Kats, and S. Ben-Yaakov, An RC load model of parallel and series-parallel resonant DC-DC converters with capacitive output filter, *IEEE Trans. Power Electron.*, 14(3), 1999, 515–521.
- [35]. R P Severns, Topologies for three-element resonant converters, *IEEE Trans. Power Electron*, 7(1), 1992, 89–98